Epitaxial Heusler alloy Co_2FeSi/GaAs(001) hybrid structures

M. Hashimoto, J. Herfort, H.-P. Schönherr, and K. H. Ploog
Paul-Drude-Institut für Festkörperelektronik, Hausvogteiplatz 5-7, D-10117 Berlin, Germany

(Received 15 April 2005; accepted 19 July 2005; published online 1 September 2005)

We found that Co_2FeSi layers on GaAs(001) grown by molecular-beam epitaxy with high crystal and interface perfection as well as smooth surfaces can be obtained in the low-growth-temperature regime. The layers are thermally robust up to 250 °C. They have long-range order and crystallize in the Heusler-type $L2_1$ structure. The easy axis of magnetization is along the [110] direction caused by a dominating uniaxial in-plane magnetic anisotropy component which has an easy axis different from that of the magnetocrystalline anisotropy component. © *2005 American Institute of Physics*. [DOI: 10.1063/1.2041836]

Spintronics is a recently emerging field of new device concepts which is based on the spin degree of freedom of the electron, and is expected to lead to dramatic improvements in device performance. One of the key issues for the realization of spintronic devices is the efficient electrical injection of spin-polarized carriers into semiconductors. Electrical spin injection has been investigated mainly from Mn-doped III-V and II-VI semiconductors[1,2] and from conventional ferromagnetic metals.[3–7] Recently, Heusler alloys are of increasing interest as a candidate for a spin injection source into semiconductors, because of their high Curie temperature, their compatibility with compound and element semiconductors and half-metallicity predicted for some Heusler alloys.[8–11] There are a few reports of epitaxial Heusler alloys grown on semiconductor substrates, e.g., the full-Heusler alloys Co_2MnX,[12,13] and Ni_2MnY,[14,15] as well as the half-Heusler alloy NiMnSb.[16,17] However, no evidence of a high degree of spin-polarization as expected from theory has been observed in Heusler alloy films up to now: around 60% at maximum.[18–20]

In ferromagnet/semiconductor (FM/SC) heterostructures, mainly two obstacles with respect to their crystal structure are considered to prevent efficient electrical spin injection. One is the existence of interfacial compounds formed by diffusion of As and/or Ga into the FM layers, resulting in spin-flip scattering at the interface. The second is atomic disorder, such as vacancies, antisites and atomic swaps. This disorder introduces minority gap states and it was reported that only a few percent of antisite disorder can destroy the half-metallic nature of Heusler alloys.[21] Therefore, a highly atomically-ordered, stoichiometric and thermally stable thin film is needed for spin injection sources.

In this letter, we present our results on the fabrication and characterization of single-crystal Heusler alloy Co_2FeSi/GaAs(001) hybrid structures grown by molecular beam epitaxy (MBE). Co_2FeSi is a member of full-Heusler alloys with the cubic $L2_1$ crystal structure consisting of 4 interpenetrating fcc sublattices.[22] The lattice constant of bulk Co_2FeSi is 5.658 Å,[23] closely lattice matched to GaAs (a_{GaAs}=5.653 Å), and the lattice mismatch is as small as 0.08%. $Fe_{3-x}Co_xSi$ crystallizes in the cubic fcc structure in a wide range of x ($0<x<2.15$).[23] This phase stability allows us to control the magnetic properties, e.g., magnetic anisotropy and magnetic moment. Bulk Co_2FeSi with a large magnetic moment (5.91 μ_B at 10.2 K) is ferromagnetic up to more than 980 K,[23] which is one of the highest Curie temperature among the reported Heusler alloys. In addition, according to a band structure calculation, Co_2FeSi is located at a slightly deviated position from the Slater-Pauling curve which half-metallic Heusler alloys expected to obey. Therefore, one could expect relatively high spin-polarization degree for Co_2FeSi.[10]

In preparation of the Co_2FeSi growth, the growth conditions of the binary alloy $Co_{0.66}Fe_{0.34}$ (bcc structure) were optimized. The composition of $Co_{0.66}Fe_{0.34}$ layers was determined by comparing their lattice constant with literature data,[24] taking into account the tetragonal distortion of the layers. Then Si was added and incorporated to obtain ternary Co_2FeSi, while the Fe and Co fluxes were kept constant at the optimized amounts. Before the growth of the Co_2FeSi layers, 100 nm-thick-GaAs templates were prepared in the III-V growth chamber using standard GaAs growth conditions. As-terminated $c(4\times4)$ reconstructed GaAs (001) surfaces were prepared to prevent the formation of macroscopic defects on the surface,[25] by cooling the samples down to 420 °C under As_4 pressure. The samples were then transferred to the As-free deposition chamber under UHV of a base pressure of 5×10^{-10} Torr. The growth temperature for the Co_2FeSi layers was varied in the range 100–400 °C to find the optimum growth temperature regime. A low growth rate of about 0.1 nm/min was chosen in order to avoid the degradation of the crystal quality at these low growth temperatures. The Si cell temperature (T_{Si}) was varied from 1280 °C to 1335 °C to find the stoichiometric composition of Co_2FeSi. The thickness of the layers was determined by high-resolution x-ray diffraction (HRXRD) and x-ray reflectivity (XRR) measurements and it varies in the range from 17 nm to 23 nm in accordance with the increase of T_{Si}. The growth was *in situ* monitored using reflection high-energy electron diffraction (RHEED). The RHEED patterns of the Co_2FeSi layers show fourfold symmetric, streaky patterns with Kikuchi lines and Laue circle, indicating a two-dimensional growth mode and rather flat surfaces.

The structural properties of the films were examined *ex situ* by HRXRD with a PANalytical X'pert diffractometer using Cu K_α radiation with a Ge(220) monochrometer and an triple-bounce analyzer crystal. Figure 1 shows the results of HRXRD ω-2θ curves for Co_2FeSi(004) and $Co_{0.66}Fe_{0.34}$(002) reflections together with the simulation using the Takagi-Taupin formalism. The examined films were

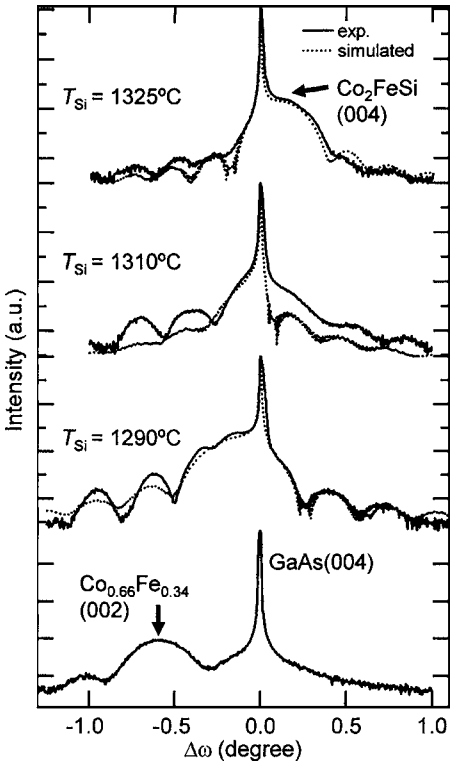

FIG. 1. Normalized ω-2θ curves for Co_2FeSi/GaAs(001) and $Co_{0.66}Fe_{0.34}$/GaAs(001) (bottom line) films grown at 100 °C with various Si cell temperatures together with the simulated curve using the Takagi-Taupin formalism (dotted lines).

grown at 100 °C with different T_{Si} (i.e., different Si composition) between 1290 °C and 1325 °C. The Co_2FeSi(004) peak systematically shifts to larger angle as T_{Si} increases up to 1325 °C, demonstrating the incorporation of Si atoms into the proper lattice sites and the formation of the ternary Co_2FeSi alloy. Distinct interference (Pendellösung) fringes are observed up to T_{Si}=1325 °C, indicating a high crystal quality, interface perfection as well as smooth surface. The smoothness of the films were further confirmed by both atomic force microscopy and XRR, and the rms surface roughness of the films turned out to be less than 1 nm for the examined films, being consistent with the results of HRXRD. To confirm the Heusler-type $L2_1$ structure, additional reflection, namely (113) reflection was recorded. Note that the (004) reflection is the principle reflection which is not influenced by disorder and the (113) is the order-dependent superlattice reflection of $L2_1$ structure.[22] The (113) reflection was clearly observed with interference fringes (not shown here), suggesting the presence of long-range atomic-ordering and the Heusler-type $L2_1$ structure.

From the perpendicular lattice mismatch $(\Delta a/a)_\perp$, the lattice constant of the layers (a_{Co_2FeSi}) was estimated and plotted as a function of T_{Si} in Fig. 2. The broken and dashed lines indicate the lattice constant of bulk Co_2FeSi and GaAs, respectively. To estimate a_{Co_2FeSi}, the tetragonal distortion of the layer, confirmed in a reciprocal space map at Co_2FeSi(113) reflections, was taken into account to obtain the unstrained parameters using the elastic constants of Fe_3Si, C_{11}=219 GPa and C_{12}=143 GPa (Ref. 26) as approximate values. The lattice constant decreases linearly with increasing T_{Si}. From a comparison with the bulk value, the stoichiometric composition of Co_2FeSi was determined.

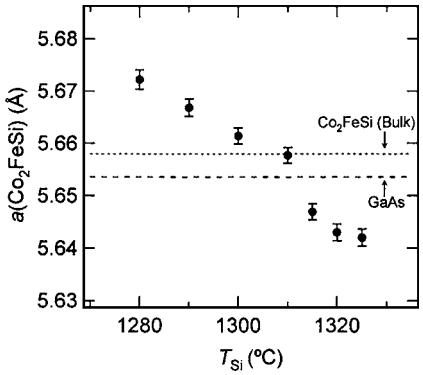

FIG. 2. Dependence of the unstrained lattice constant of Co_2FeSi layers (a_{Co_2FeSi}) on Si cell temperature. The broken line and the dashed line indicate the bulk value of Co_2FeSi and GaAs, respectively.

Figure 3 shows the results of HRXRD ω-2θ curves around (004) reflections of Co_2FeSi layers near stoichiometry grown at different temperatures between 100 °C and 350 °C. In the lower growth temperature regime, high orders of interference fringes (up to fifth order) are seen, while in T_G>250 °C the interference fringes become less pronounced, indicating the onset of crystal degradation. At T_G =350 °C, the main peak is broadened and shifted to larger angle. This peak broadening and shift with increasing T_G has also been observed in our study on Fe_3Si/GaAs(001) (Ref. 27) and is most likely due to interfacial reaction or phase separation. This is further evidenced by the wide-range ω-2θ scans with a wide-open detector for the same series of samples (not shown here). An additional peak appeared at around ω=17.3° for the sample grown at 350 °C. We ascribe this peak to either $Co_{1-x}Fe_xSi_2$(002) caused by phase separation or $(Co,Fe)_2As$(110) by interfacial reaction. Therefore, the optimum growth temperature range of Co_2FeSi at which good crystal and interface quality can be obtained is T_G <250 °C. It should be stressed that in terms of thermal stability, Co_2FeSi is much more suitable for device applications than Fe, Co and FeCo on GaAs, for which interfacial reac-

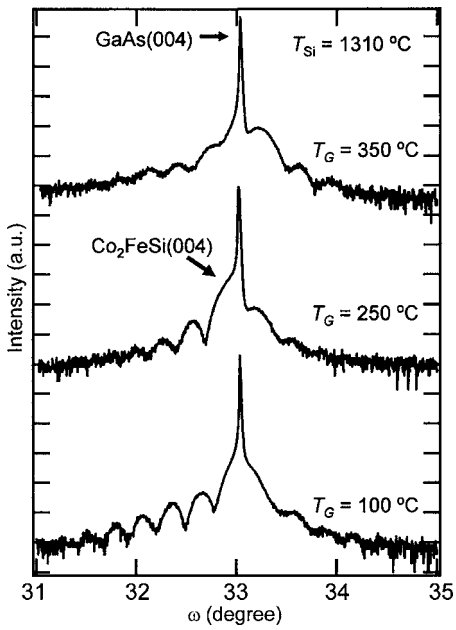

FIG. 3. Normalized ω-2θ curves for stoichiometric Co_2FeSi/GaAs(001) films grown at various growth temperature ranging from 100 °C to 350 °C.

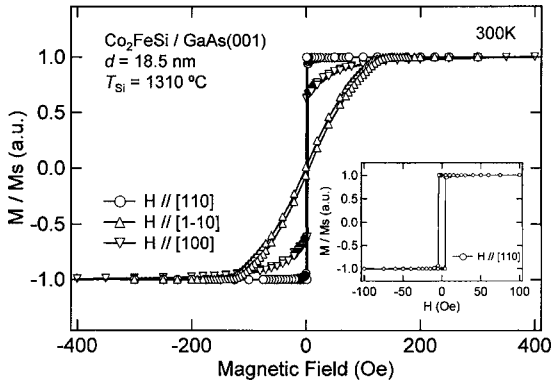

FIG. 4. Magnetization curves for 18.5 nm thick stoichiometric $Co_2FeSi/GaAs(001)$ film grown at 100 °C. The inset shows an expanded view of the magnetization curve along the [110] direction. After subtraction of the diamagnetic contribution of the GaAs substrate, the magnetizations were normalized to the saturation magnetization in each direction.

tions occur at much lower T_G.[25] However, since it is very difficult to detect nano meter-size interfacial compounds or clusters by XRD, detailed transmission electron microscopy studies are in preparation for this system.

The magnetic properties of Co_2FeSi were investigated using superconducting quantum interference device (SQUID) magnetometry at room temperature. The external magnetic field was applied along the [110], [1$\bar{1}$0], and [100] directions. All the examined $Co_{2-x}Fe_{1-y}Si_{1+x+y}$ films are ferromagnetic at room temperature and have the same easy axis of magnetization ([110] direction). Figure 4 shows the magnetization curves of the stoichiometric Co_2FeSi film grown at 100 °C and an expanded view along the [110] direction in the inset. The magnetization curves show an easy axis [110], a hard axis [1$\bar{1}$0], and an intermediate axis [100]. The magnetization curve along [110] shows a square-shaped hysteresis loop with a small coercive field of 4.5 Oe, indicating excellent crystal quality. The saturation magnetization of stoichiometric films amounts to 1250 ± 120 emu/cm^3, which is relatively close to that of bulk Co_2FeSi [1124 emu/cm^3 at 295 K (Ref. 23)], confirming the stoichiometric composition determined by HRXRD.

The easy axis of $Co_2FeSi/GaAs$ ([110] direction) is inconsistent with that expected from the magnetocrystalline anisotropy and found in other Heusler alloys like $Fe_3Si/GaAs$ ($\langle 100\rangle$ directions).[27] The discrepancy can be explained by an analysis of the in-plane magnetic anisotropy assuming two anisotropy components, the cubic magnetocrystalline anisotropy, and the uniaxial anisotropy. The effective value of the uniaxial and cubic magnetocrystalline anisotropy constants (K_u^{eff} and K_1^{eff}, respectively) for the stoichiometric Co_2FeSi film ($d=18.5$ nm) were obtained by fitting the magnetization curves along the [1$\bar{1}$0] direction using the method described by Dumm *et al.*[28] We found $K_1^{\text{eff}}=1.8\times10^4$ emu/cm^3 and $K_u^{\text{eff}}=6.3\times10^4$ erg/cm^3, respectively. These two anisotropy constants have the same sign, however they do not share the same easy axis; $\langle 100\rangle$ and [110] directions for the cubic and the uniaxial component, respectively. As a result of the dominating uniaxial component, the easy axis in total is modulated to the [110] direction. The origin of the relatively large K_u^{eff} value despite the rather large film thickness is not yet clear. We believe that K_u^{eff} is a pure interface-related term originating from an anisotropic bonding at the FM/SC interface as has been found in other FM/SC systems.[29]

In conclusion, we have grown single-crystal Heusler alloy $Co_2FeSi/GaAs(001)$ hybrid structures by molecular beam epitaxy. Co_2FeSi layers with high crystal and interface perfection as well as smooth surfaces can be obtained by carefully controlling the fluxes of Co, Fe, and Si. The high crystal and interface perfection is preserved up to growth temperature of 250 °C, being thus much more thermally stable than conventional ferromagnetic metals on GaAs.

[1] R. Fiederling, M. Keim, G. Reuscher, W. Ossau, G. Schmidt, A. Waag, and L. W. Molenkamp, Nature (London) **402**, 787 (1999).
[2] Y. Ohno, D. K. Young, B. Beschoten, F. Matsukura, H. Ohno, and D. D. Awschalom, Nature (London) **402**, 790 (1999).
[3] H. J. Zhu, M. Ramsteiner, H. Kostial, M. Wassermeier, H.-P. Schönherr, and K. H. Ploog, Phys. Rev. Lett. **87**, 016601 (2001).
[4] B. T. Jonker, A. T. Hanbicki, Y. D. Park, G. Itskos, M. Furis, G. Kioseoglou, A. Petrou, and X. Wei, Appl. Phys. Lett. **79**, 3098 (2001).
[5] X. Jiang, R. Wang, S. van Dijken, R. Shelby, R. Macfarlane, G. S. Solomon, J. Harris, and S. S. P. Parkin, Phys. Rev. Lett. **90**, 256603 (2003).
[6] T. Manago and H. Akinaga, Appl. Phys. Lett. **81**, 694 (2002).
[7] A. Kawaharazuka, M. Ramsteiner, J. Herfort, H.-P. Schönherr, H. Kostial, and K. H. Ploog, Appl. Phys. Lett. **85**, 3492 (2004).
[8] C. Palmstrøm, MRS Bull. **28**, 725 (2003).
[9] R. A. de Groot, F. M. Mueller, P. G. van Engen, and K. H. J. Buschow, Phys. Rev. Lett. **50**, 2024 (1983).
[10] I. Galanakis, P. H. Dederichs, and N. Papanikolaou, Phys. Rev. B **66**, 174429 (2002).
[11] S. Fujii, S. Sugimura, Ishida, and S. Asano, J. Phys.: Condens. Matter **2**, 8583 (1990).
[12] T. Ambrose, J. J. Krebs, and G. A. Prinz, Appl. Phys. Lett. **76**, 3280 (2000).
[13] S. N. Holmes and M. Pepper, Appl. Phys. Lett. **81**, 1651 (2002).
[14] J. Q. Xie, J. W. Dong, J. Lu, C. J. Palmstrøm, and S. Mckernan, Appl. Phys. Lett. **79**, 1003 (2001).
[15] M. S. Lund, J. W. Dong, J. Lu, X. Y. Dong, C. J. Palmstrøm, and C. Leighton, Appl. Phys. Lett. **80**, 4798 (2002).
[16] W. Van Roy, J. De Boeck, B. Brijs, and G. Borghs, Appl. Phys. Lett. **77**, 4190 (2000).
[17] P. Bach, A. S. Bader, C. Rüster, C. Gould, C. R. Becker, G. Schmidt, L. W. Molenkamp, W. Weigand, C. Kumpf, E. Umbach, R. Urban, G. Woltersdorf, and B. Heinrich, Appl. Phys. Lett. **83**, 521 (2003).
[18] S. Kämmerer, A. Thomas, A. Hütten, and G. Reiss, J. Appl. Phys. **85**, 79 (2004).
[19] L. J. Singh, Z. H. Barber, Y. Miyoshi, W. R. Branford, and L. F. Cohen, J. Appl. Phys. **95**, 7231 (2004).
[20] R. J. Soulen Jr., J. M. Byers, M. S. Osofsky, B. Nadgorny, T. Ambrose, S. F. Cheng, P. R. Broussard, C. T. Tanaka, J. Nowak, J. S. Moodera, A. Barry, and J. M. D. Coey, Science **282**, 85 (1998).
[21] S. Picozzi, A. Continenza, and A. J. Freeman, Phys. Rev. B **69**, 094423 (2004).
[22] For the details of the $L2_1$ structure, see P. J. Webster and K. R. A. Ziebeck, *Landolt-Börnstein New Series III/19c* (Springer, Berlin, 1988), p. 75.
[23] V. Niculescu, J. I. Budnick, W. A. Hines, K. Raj, S. Pickart, and S. Skalski, Phys. Rev. B **19**, 452 (1979).
[24] T. Nishizawa and K. Ishida, Bull. Alloy Phase Diagrams **5**, 250 (1984).
[25] H.-P. Schönherr, R. Nötzel, W. Ma, and K. H. Ploog, J. Appl. Phys. **89**, 169 (2001).
[26] G. Kötter, K. Nembach, F. Wallow, and E. Nembach, Mater. Sci. Eng., A **114**, 29 (1989).
[27] J. Herfort, H.-P. Schönherr, and K. H. Ploog, Appl. Phys. Lett. **83**, 3912 (2004); J. Herfort, H.-P. Schönherr, K.-J. Friedland, and K. H. Ploog, J. Vac. Sci. Technol. B **22**, 2073 (2004).
[28] M. Dumm, M. Zölfl, R. Moosbühler, M. Brockmann, T. Schmidt, and G. Bayreuther, J. Appl. Phys. **87**, 5457 (2000).
[29] E. Sjöstedt, L. Nordström, F. Gustavsson, and O. Eriksson, Phys. Rev. Lett. **89**, 267203 (2002).